A novel fluorine relaxation switch for tracking the binding and intracellular processing of molecularly targeted nanoparticle contrast agents

L. Hu[1], J. Chen[1], S. D. Caruthers[1], G. M. Lanza[1], and S. A. Wickline[1]
[1]Washington University in St. Louis, St. Louis, MO, United States

Introduction: In the field of molecular imaging with nanoparticle contrast agents, it would be advantageous to know not only that a particle binds to its target but also that it is internalized and subsequently processed and sorted to the subcellular compartment [1]. One class of contrast agents, paramagnetic perfluorocarbon (PFC) nanoparticles (NP) [2], features a strong local ^{19}F-Gd interaction that is highly dependent on the spatial separation between these two compounds, which allows the use of ^{19}F relaxation to assess the binding and unpacking of NP by the cell. Here we develop an analytical description and experimental validation of ^{19}F longitudinal T1 relaxation as an indicator for assessing the integrity of paramagnetic PFC NP. When Gd is stripped from the nanoparticle surface, a "relaxation switch" occurs revealing the transition from intact bound particle to processed constituents.

Method: *1) NP formulation.* PFC NP are created by adding a lipid-anchored, chelated Gd compound (100,000-200,000 copies per particle) into the lipid monolayer surrounding a liquid perfluorocarbon core to form a nanoparticle of diameter ~ 250 nm (Fig.1a). A peptidomimetic $\alpha_v\beta_3$-integrin antagonist was anchored to the lipid membrane for targeted binding of PFC NP to cells expressing $\alpha_v\beta_3$-integrin. 2) *Mathematical model and experimental validation.* The analytic expression for ^{19}F longitudinal relaxation enhancement of PFC caused the external Gd coating was derived based on Solomon, Bloembergen and Morgan (SBM) theory [3],

$$\Delta R_1 = \frac{3}{2}\hbar^2\gamma_I^2\gamma_S^2 S(S+1)C_1\frac{[Gd]}{r}\int_0^\infty \frac{Dk^3}{\omega_I^2+(Dk^2)^2}\left[\int_d^\infty \frac{J_{5/2}(kx)}{x^{3/2}}\left(1-\frac{d}{x}\right)dx\right]^2 dk \quad , \qquad (1)$$

in which [*Gd*] is the Gd ions to lipid ratio, *r* is particle size, *D* is the free diffusion coefficient of PFC, *d* is the "distance of closest approach" for PFC to move toward Gd, ω_I is the Lamor frequency of ^{19}F, γ_I and γ_S are the gyromagnetic ratios for relevant nuclear and electron spin, *S* is the quantum number of electron spin of Gd and C_1 is a constant for normalization. The structural parameters of NP are depicted in Fig. 1a. Because the contact interaction between ^{19}F and Gd is prevented by the surrounding monolipid layer, the relaxation is purely outer-sphere in nature. To test the theoretical prediction, we measured the size, diffusion coefficient of PFC molecule and nuclear magnetic resonance dispersion (NMRD) curve at several MRI related fields for three kinds of paramagnetic PFC NP. The "distance of closest of approach" of ^{19}F to Gd ions was fitted from the experimental data with non-linear regression. *3) In vitro application*. Cultured macrophage cells (RAW 267.7 cell line) that express $\alpha_v\beta_3$-integrin were treated with perfluoro-15-crown-5 ether (CE) NP anchored with DTPA-BOA-Gd (2 µl/ml). After 2, 24 and 48 hour's incubation, cells were washed with PBS 3 times and then centrifuged in a pellet. ^{19}F spectroscopic quantification was performed at an 11.7 T Varian small animal imaging scanner using previously reported methods [4]. The ^{1}H and ^{19}F relaxation properties of cells were measured at a 4.7 T Varian small animal imaging scanner. To confirm that other factors, e.g. intracellular oxygenation, do not contribute to the change of ^{19}F T1 after internalization, the ^{19}F T1 of cell internalized plain CE NP was also measured.

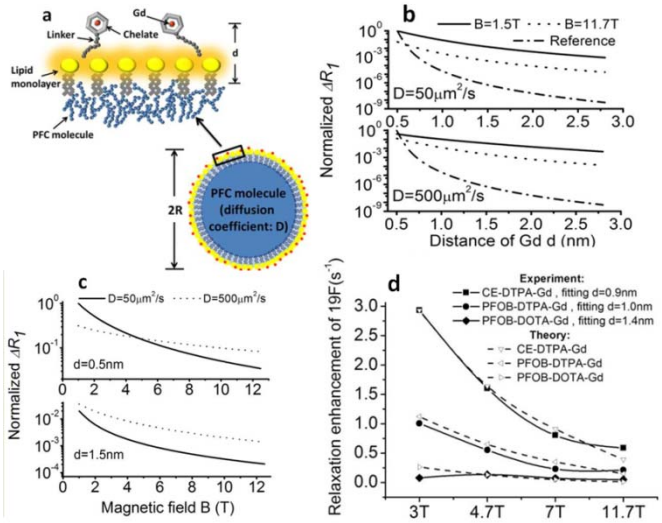

Figure 1. (a) Illustration of configuration of paramagnetic PFC NP. (b&c) Normalized relaxation enhancement as a function of "distance of closest approach" *d* and external field strength *B*. The reference is the curve $1/d^6$, the distance dependence of magnetic dipolar interaction on separation of two dipoles. (d) The theoretical prediction is confirmed by experimentally measured ^{19}F relaxation enhancement on three types of Gd loaded NP.

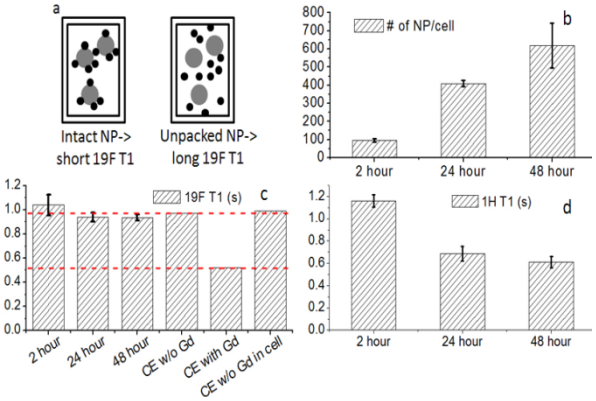

Figure 2. (a) Longitudinal relaxation reflects the integrity of internalized paramagnetic PFC NP. (b-d) number of NP and ^{1}H/^{19}F T1 of PFC labeled cells after 2, 24, 48 hour's incubation.

Results: Figure 1b&c shows the predicted ^{19}F relaxation enhancement of paramagnetic PFC NP as a function of "distance of closest approach" and external field strength. For three types of PFC NPs (i.e., CE core with DTPA-BOA-Gd, PFOB core with DTPA-BOA-Gd and DOTA-PE-Gd), the fitted "distance of closest approach" from experimental data confirms that DTPA-BOA-Gd has a shorter linker chain than DOTA-PE-Gd [4]. After treating macrophages with Gd-DTPA coated PFC NP, quantitative ^{19}F MRS shows the number of PFC NP per cell increased progressively within the first 48 hours. The delivery of PFC NP to macrophage cells was also confirmed by the progressively decreased ^{1}H T1 reflecting paramagnetic effect of Gd. The ^{19}F T1 of PFC NP, however, was recovered to the baseline value of plain PFC NP (i.e., without Gd coating) after endocytosis. The shortened ^{1}H T1 but recovered ^{19}F T1 suggested that Gd chelates have been separated from PFC NP upon delivery to macrophage cells.

Discussion and Conclusion: Our theoretical modeling and experimental results showed that the paramagnetic effect Gd on ^{19}F T1 relaxation was most effective when Gd is anchored on the PFC NP surface and at relatively low magnetic field. The absence of this ^{19}F T1 shortening effect could provide a sensitive indicator to detect the separation of Gd from PFC NP. Further combining with ^{1}H T1 measurements represented an effective technique to monitor the binding, unpacking, and the subsequent distribution of PFC NP and its payloads.

References: [1] K. C. Partlow, et al, Biomaterial, 29: 3367 (2008). [2] A. M. Neubauer, et al., MRM 60:1066 (2008). [3] Solomon I, Physical Review 99559-565 (1955). [4] Richard Southworth, el at., Nanomedicine 5:359 (2009). [5] P. Winter, et al, JMMM, 293: 540 (2005). [6] S. H. Koenig, et al, MRM, 22: 183 (1991).